

Araştırma Makalesi / Research Article

Synthesis and Characterization of a New Nickel(II) Compound Derived from $[BW_{12}O_{40}]^{3-}$ and 2,2'-BipyridylMükerrem FİNDİK^{1*}, Asuman UÇAR², Nuriye KOÇAK³, Onur ŞAHİN⁴, Alper Tolga ÇOLAK⁵¹Necmettin Erbakan University, A.K. Education Faculty, Department of Chemistry Education, Research Laboratory, Konya, Turkey.²Agri Ibrahim Cecen University, Education Faculty, Department of Science Education, Agri, Turkey.³Necmettin Erbakan University, A.K. Education Faculty, Department of Science Education, Konya, Turkey.⁴Sinop University, Department of Scientific and Technological Research Application and Research Center, Sinop, Turkey.⁵Dumlupınar University, Faculty of Arts and Science, Department of Chemistry, Kutahya, Turkey.* Sorumlu yazar e-posta: mmukerrem@gmail.com. ORCID ID: <https://orcid.org/0000-0002-9441-0814>e-posta: asucar340@gmail.com. ORCID ID: <https://orcid.org/0000-0003-2674-3120>e-posta: nuriye42@gmail.com. ORCID ID: <https://orcid.org/0000-0002-0531-3538>e-posta: onurs@sinop.edu.tr. ORCID ID: <https://orcid.org/0000-0003-3765-3235>e-posta: atahan2005@gmail.com. ORCID ID: <https://orcid.org/0000-0003-4478-7792>

Geliş Tarihi: 01.07.2020

Kabul Tarihi: 31.08.2020

Abstract**Keywords**
Keggin-type;
Polyoxometalate;
Crystal structure; 2,2'-
bipyridyl

A Keggin-type polyoxometalate $\{Ni(2,2'-bipy)_2(H_2O)[BW_{12}O_{40}]\}^{3-}$ (NiBWO) has been hydrothermally synthesized in the high temperature resistant glass bottle for the first time. The structure has been characterized by elemental analyses, X-ray diffraction, Fourier Transform Infrared Spectroscopy, Thermogravimetric Analysis, Scanning Electron Microscope and X-ray single crystal diffraction analyses. The X-ray single crystal study shows that the asymmetric unit of NiBWO is composed of one $[BW_{12}O_{40}]^{5-}$ anion, one $[Ni(2,2'-bipy)_2(H_2O)]^{2+}$ and one and a half of $[Ni(2,2'-bipy)_3]^{2+}$ cations.

 $[BW_{12}O_{40}]^{3-}$ ve 2,2'-Bipiridil İçeren Yeni Bir Nikel(II) Kompleksinin Sentezi ve Karakterizasyonu**Öz****Anahtar Kelimeler**
Keggin-
tipPolioksometalat;
Kristal yapı; 2,2'-
bipiridil.

Keggin tipi bir polioksometalat olan $\{Ni(2,2'-bipy)_2(H_2O)[BW_{12}O_{40}]\}^{3-}$ (NiBWO) bileşiği yüksek ısıya dayanıklı cam şişede hidrotermal olarak ilk kez sentezlenmiştir. Bileşiğin yapısı elementel analiz, X-ışını kırınımı, Fourier Dönüşümlü Kızılötesi Spektroskopisi, Termogravimetrik Analiz, Taramalı Elektron Mikroskobu ve X-ışını tek kristal kırınım analizleri ile karakterize edilmiştir. X-ışını tek kristal analiz sonucu, NiBWO bileşiğinin asimetrik biriminin bir $[BW_{12}O_{40}]^{5-}$ anyonu, bir $[Ni(2,2'-bipy)_2(H_2O)]^{2+}$ ve bir buçuk $[Ni(2,2'-bipy)_3]^{2+}$ katyonlarından oluştuğunu göstermiştir.

© Afyon Kocatepe Üniversitesi

1. Introduction

The oxoanions containing multiple metal atoms are called polyoxometalates or POMs and have been known since the early 19th century. Berzelius synthesized the ammonium salt of $PMo_{12}O_{40}^{3-}$ anion, the first compound of the POM class, in 1826 (Berzelius 1826). From then on, researchers have synthesized POMs in new forms with different

metals. Hybrid inorganic-organic materials are synthesized for acquiring new materials with properties and bespoke structures. The most remarkable advantage of hybrid inorganic-organic materials are that they can combine dissimilar properties of inorganic and organic components in one material (Zhang et al. 2008, Kastner et al. 2017, Cameron et al. 2018). POM compounds becoming

hybrid compounds with the added metals and the organic ligand into their structure are employed in the surface science studies (Shakeri et al. 2019), the preparation of amphiphilic molecules (Zhao et al. 2019), the production of catalytic materials (Findik et al. 2019), the manufacture of medical supplies (Zong et al. 2018), and the continuous development are observed in the field of potential applications of these compounds.

It is well-known that transition-metal-substituted polyoxometalates are of great interest in the last decades owing to their controlled structures. The physical and chemical properties of different structures are applicable to diverse areas, such as magnetism, optics, catalysis, sensor, luminescence and materials science (Zheng et al. 2007, Zheng et al. 2012, Huang et al. 2014). Our aim in this study is to synthesize structures that serve as a new model for the design and formation of transition-metal-substituted POM architectures.

In this paper, we reported a new hybrid compound based on Keggin polyoxometalate. {Ni(2,2'-bipy)₂(H₂O)[BW₁₂O₄₀]}³⁻ (NiBWO) is composed of one [BW₁₂O₄₀]⁵⁻ anion, one [Ni(2,2'-bipy)₂(H₂O)]²⁺ and one and a half of [Ni(2,2'-bipy)₃]²⁺ cations: The structure of the synthesized compound was characterized by Fourier Transform Infrared Spectroscopy (FT-IR), elemental analyses, X-ray diffraction (XRD), Thermogravimetric Analysis (TGA), Scanning Electron Microscope (SEM) and X-ray single crystal diffraction analyses.

2. Materials and Methods

2.1. Chemicals

Nickel(II)chloride hexahydrate (NiCl₂.6H₂O) and hydrochloric acid (HCl) were supplied by Merck. Sodium tungstate dehydrate (Na₂WO₄.2H₂O), boric acid (H₃BO₃), 2,2'-bipyridyl (2,2'-bipy) and perchloric acid (HClO₄) were supplied by Sigma-Aldrich.

2.2. Apparatus

Perkin-Elmer 2400 CHN elemental analyzer was used for elemental analysis (C, N and H) of sample. For structural analysis of the sample was measured in the range of 4000 to 500 cm⁻¹ using Attenuated Total Reflection-Fourier Transformed Infrared (ATR-FTIR) spectrometer (Perkin Elmer 100). XRD using a

Bruker axis diffractometer (Bruker D8 ADVANCE) was used for the determination of the crystal structure of the NiBWO. The parameters of Bruker axis diffractometer was CuK α radiation, operating at 40 kV and 30 mA with a rate of 21°/min. Setaram thermal gravimetric analyzer was used for thermogravimetric analysis of the NiBWO over the temperature range of 25–1000 °C under a heating ramp of 10 °C min⁻¹ at N₂ atmosphere. SEM image was taken on a Hitachi – SU 1510 at accelerating voltage of 20 kV and magnification of 10.00 kX.

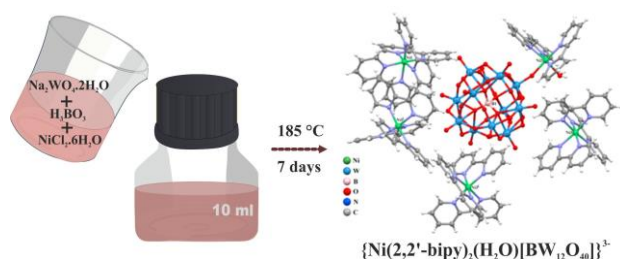
The hydrogen atoms bound to carbon atoms were treated as riding atoms with distances of 0.93 Å. Other H atoms were refined freely. In order to avoid ADP and NPD problems, the EADP command was used to refine the non-H atoms. With SHELXS-2013 (Sheldrick 2008), the structure of NiBWO was solved by direct methods and refined using full-matrix least-squares methods with SHELXL-2013 program (Sheldrick 2015) within WinGX (Farrugia 1999). The structural data of NiBWO was collected on Bruker APEX2 (Bruker 2013). MERCURY program was used for molecular graphics. Details of data collection and crystal structure determinations are shown in Table 1. Crystallographic data of the structure has been deposited in the Cambridge Crystallographic Data Center with CCDC number 1497303.

2.3. Procedure

In the synthesis of the new type of polyoxometalate, a new low cost method is used other than the traditional synthesis of polyoxometalates. In this method, instead of Teflon-lined autoclave, special production bottles and caps resistant to high temperatures are used. Schematic representation of the synthesis of NiBWO is given Scheme 1.

An aqueous solution of H₃BO₃ (1.5 mmol, 0.093 g), Na₂WO₄.2H₂O (3.00 mmol, 0.99 g), NiCl₂.6H₂O (0.825 mmol, 0.196 g) and 2,2'-bipy (0.75 mmol, 0.117 g) was stirred at room temperature for one hour. 6 M HCl was added to the mixture to adjusted the pH to 1.15, then the mixture transferred in a 10 mL bottle and allowed to react at 185 °C. After seven days, the product was slowly cooled down to room temperature at a rate of 10 °C/h, pink crystals were collected by filtration, washed several times with distilled water, and dried in air (yield 59%, based on

W). Elemental analysis (%): Calcd: $C_{130}H_{108}B_2N_{26}Ni_5O_{82}W_{24}$: C, 19.34; N, 4.51; H, 1.34; Found: C, 19.43; N, 4.57; H, 1.40. FT-IR (cm^{-1}): 3079, 1598, 1472, 1441, 1021, 948, 876, 754.



Scheme 1. Schematic representation of the synthesis of NiBWO.

3. Results and Discussion

3.1. Crystal structure

According to the result of X-ray single crystal study, the asymmetric unit of NiBWO has been proved to consist of one $[BW_{12}O_{40}]^{5-}$ anion, one $[Ni(2,2'-bipy)_2(H_2O)]^{2+}$ and one and a half of $[Ni(2,2'-bipy)_3]^{2+}$. $[BW_{12}O_{40}]^{5-}$ anion with a Keggin-type structure has a structure with a central BO_4 [B-O bond distances range of 1.53(5)–1.56(6) Å] surrounded by the $W_{12}O_{36}$ group with tetrahedron coordination geometry. The presence of the two types of Ni(II) complexes $\{[Ni(2,2'-bipy)_2(H_2O)]^{2+}$ and $[Ni(2,2'-bipy)_3]^{2+}\}$ is the most striking feature of NiBWO (Figure 1). Each Ni(II) atoms of $[Ni(2,2'-bipy)_3]^{2+}$ coordinated by six nitrogens from three 2,2'-bipy ligands [Ni-N bond lengths range of 2.02(4)–2.15(4) Å], showing a distorted octahedral geometry. The Ni2 atom is coordinated by four nitrogens from two 2,2'-bipy ligands [Ni-N bond lengths range of 2.01(4)–2.12(4) Å], one oxygen from a coordinated water molecule [Ni-O = 2.12(3) Å] and one oxygen from an anion $[BW_{12}O_{40}]^{5-}$ [Ni2-O40 = 2.03(3) Å], exhibiting a different distorted octahedral geometry. In other words, $[Ni(2,2'-bipy)_2(H_2O)]^{2+}$ should actually be described as $\{Ni(2,2'-bipy)_2(H_2O)[BW_{12}O_{40}]\}^{3-}$ (Figure 1). Selected bond lengths for NiBWO (Å) are shown in Table 2.

Table 1. Crystal data and structure refinement for NiBWO.

Empirical formula	$C_{130}H_{108}B_2N_{26}Ni_5O_{82}W_{24}$
Formula weight	8073.99
Crystal system	Monoclinic
Space group	C2/c
<i>a</i> (Å)	46.683 (6)
<i>b</i> (Å)	14.347 (2)
<i>c</i> (Å)	26.020 (4)
β (°)	90.001 (4)
<i>V</i> (Å ³)	17427 (4)
<i>Z</i>	4
Diffractometer	BRUKER D8-QUEST
Temperature (K)	296
θ range (°)	3.0–26.1
Measured refls.	103877
Independent refls.	17089
Parameters	271
<i>R</i> _{int}	0.176
<i>S</i>	1.13
<i>R</i> 1/ <i>wR</i> 2	0.115/0.303

Table 2. Selected bond lengths for NiBWO (Å).

B1-O1	1.53(6)	N11-Ni3	2.09(3)
B1-O2	1.56(6)	B1-O3	1.55(5)
N3-Ni1	2.04(4)	N2-Ni1	2.05(4)
N6-Ni1	2.15(4)	N5-Ni1	2.03(4)
N7-Ni2	2.05(4)	O41-Ni2	2.12(3)
N10-Ni2	2.12(4)	N9-Ni2	2.01(4)

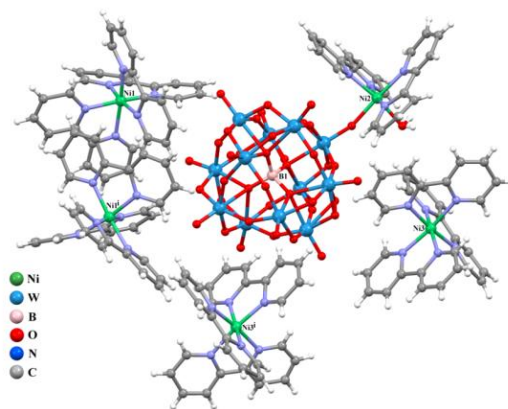
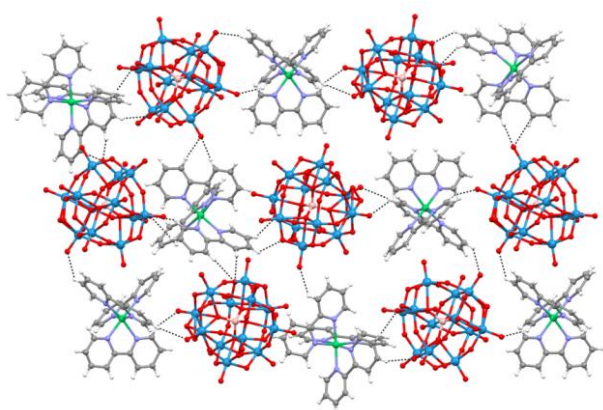
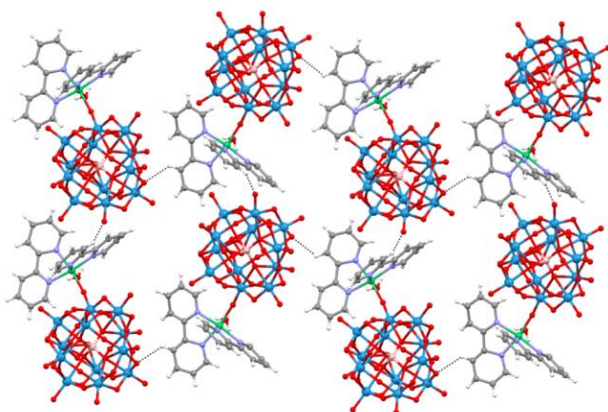


Figure 1. The molecular view of NiBWO [(i) $-x+1, y, -z+1/2$].

The complex has C–H \cdots O hydrogen bonds between POMs and $[Ni(2,2'-bipy)_3]^{2+}$ (Table 3). Figure 2 shows POMs hydrogen bonds with three $[Ni(2,2'-bipy)_3]^{2+}$ with C \cdots O lengths in the range of 3.03(3)–3.50(7) Å, respectively. Similarly, Figure 3 shows the POMs hydrogen bonds with $[Ni(2,2'-bipy)_2(H_2O)]^{2+}$, with C \cdots O lengths in the range of 3.00(8)–3.40(6) Å, respectively.

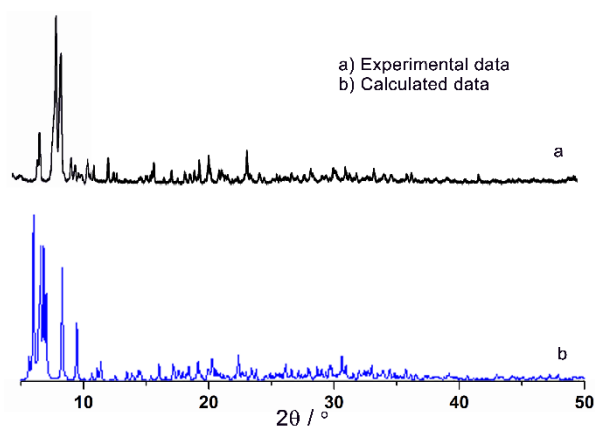
Table 3. Hydrogen-bond parameters for NiBWO (Å, °).

D-H...A	D-H	H...A	D...A	D-H...A
C2—H2...O9	0.93	2.50	3.31 (5)	146
C3—H3...O39	0.93	2.38	3.03 (3)	127
C4—H4...O34 ⁱⁱ	0.93	2.34	3.13 (7)	142
C7—H7...O34 ⁱⁱ	0.93	2.57	3.48 (5)	165
C9—H9...O9 ⁱⁱⁱ	0.93	2.56	3.18 (5)	125
C10—H10...O9 ⁱⁱⁱ	0.93	2.58	3.21 (5)	126
C14—H14...O32 ^{iv}	0.93	2.14	3.05 (6)	167
C17—H17...O32 ^{iv}	0.93	2.23	3.13 (6)	164
C31—H31...O14	0.93	2.48	3.40 (6)	172
C32—H32...O26	0.93	2.30	3.00 (8)	131
C37—H37...O8 ^v	0.93	2.52	3.13 (7)	124
C44—H44...O30 ^{vi}	0.93	2.59	3.38 (7)	144
C60—H60...O26	0.93	2.34	3.14 (10)	144
C64—H64...O27	0.93	2.60	3.50 (7)	162
C64—H64...O27 ^{vii}	0.93	2.47	3.19 (7)	134

**Figure 2.** The molecular view of hydrogen bonds between the POM and $[Ni(2,2'-bipy)_3]^{2+}$ in NiBWO.**Figure 3.** The molecular view of hydrogen bonds between the POM and $[Ni(2,2'-bipy)_2(H_2O)]^{2+}$ in NiBWO.

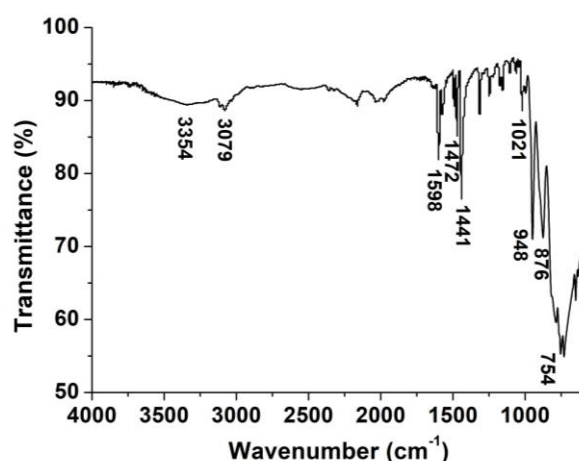
3.2. Powder X-ray diffraction

The measured XRD curve (Figure 4) gives similar results to the calculated model. This confirms the purity of the crystal product. The intensity difference may depend on the preferred direction of the powder samples.

**Figure 4.** Experimental and simulated XRD curves of NiBWO.

3.3. Infrared spectroscopy

The FT-IR spectrum of the NiBWO is shown in Figure 5. In the spectrum, the characteristic band at 948 cm^{-1} is attributed to W–Ot, the band at 876 cm^{-1} is ascribed to W–Ob–W, the band at 754 cm^{-1} is due to W–Oc and the band at 1021 cm^{-1} is ascribed to B–O. The four mentioned peaks are characteristic peaks for $[BW_{12}O_{40}]^{5-}$ (Du et al. 2019). The absorption bands at $1598\text{--}1441\text{ cm}^{-1}$ are due to vibrations of 2,2'-bipy ligand in the NiBWO (Xiao et al. 2018). 3079 cm^{-1} are attributed to the vibrations of the $\nu(\text{C-H})$ in bipy rings of the ligand (Lu et al. 2019). The peaks at ca. 3354 cm^{-1} are attributed to the vibrations of $\nu(\text{H}_2\text{O})$ (Lu et al. 2015).

**Figure 5.** FT-IR spectrum of NiBWO.

3.4. Thermogravimetric analysis

Thermal stability for the NiBWO was investigated by TGA (Figure 6). Firstly, 0.44% weight loss up to 165 °C corresponds to the separation of free water molecules. These water molecules that interact more strongly with the POM frame are separated

from 80 to 200 °C (Canioni et al. 2011). The second weight loss of 8.3% at 560 °C can be attributed to the decomposition of the 2,2'-bipy (Liu et al. 2015). The final mass loss around 880 °C (25.6%) is attributed to the complete rupture of the remainder POM cluster (Lan et al. 2013).

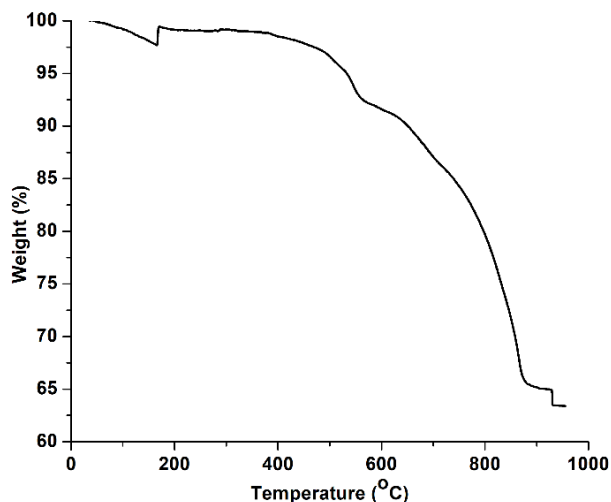


Figure 6. TGA curve of NiBWO.

3.5. SEM analysis

SEM is used to examine the three important factors surfactant morphology (surface structural properties based on shape and size), surface crystallography (ie, surface formation of atoms) and surface composition (in terms of surface composition, compounds and elements). So, the surface property of the NiBWO was checked by using SEM (Figure 7). According to the SEM image, each crystal has a cuboid structure.

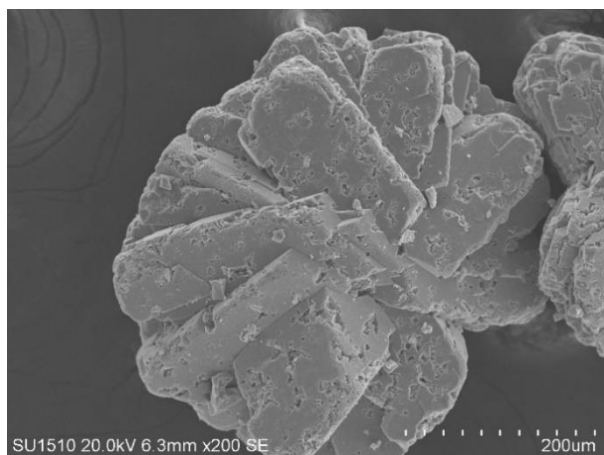


Figure 7. SEM image of NiBWO.

4. Conclusion

A new organic–inorganic hybrid, $\{Ni(2,2'-bipy)_2(H_2O)[BW_{12}O_{40}]\}^{3-}$, compound has been synthesized via a simple route under hydrothermal conditions through carefully tuning the reaction temperature. The use of high temperature bottles used in the synthesis method may be preferred by the researchers in terms of decreasing the cost in subsequent studies. The compound was characterized by X-ray diffraction method, FT-IR spectra and TGA. These analyzes support the results from the single crystal X-ray structural analysis. According to the X-ray, the compound is based on Keggin polyoxoanions.

Acknowledgement

The authors acknowledge Scientific and Technological Research Application and Research Center, Sinop University, Turkey, for the use of the Bruker D8 QUEST diffractometer. The authors thank the Necmettin Erbakan University Research Foundation (151210002).

References

- APEX2, Bruker AXS Inc. Madison Wisconsin USA 2013.
- Berzelius, J.J., 1826. Beitrag zur näheren Kenntniss des Molybdäns. *Annalen der Physik*, **82(4)**, 369–392.
- Cameron, J.M., Wales, D.J. and Newton, G.N., 2018. Shining a light on the photo-sensitisation of organic–inorganic hybrid polyoxometalates. *Dalton Transactions*, **47**, 5120–5136.
- Canioni, R., Roch-Marchal, C., Secheresse, F., Horcajada, P., Serre, C., Hardi-Dan, M., Ferey, G., Greneche, J.M., Lefebvre, F., Chang, J.S., Hwang, Y.K., Lebedev, O., Turner, S.B. and Tendeloo, G.V., 2011. Stable polyoxometalate insertion within the mesoporous metal organic framework MIL-100(Fe). *Journal of Materials Chemistry*, **21**, 1226–1233.
- Du, N., Gong, L., Fan, L., Yu, K., Luo, H., Pang, S., Gao, J., Zheng, Z., Lv, J. and Zhou, B., 2019. Nanocomposites Containing Keggin Anions Anchored on Pyrazine Based Frameworks for Use as Supercapacitors and Photocatalysts. *ACS Applide Nano Materials*, **2**, 3039–3049.
- Farrugia, L.J., 1999. WinGX suite for small-molecule single-crystal crystallography. *Journal of Applied Crystallography*, **32**, 837–838.

- Findik, M., Ucar, A., Colak, A.T., Sahin, O., Bingol, H., Sayin, U. and Kocak, N., 2019. Self-assembly of a new building block of $\{BMo_{12}O_{40}\}$ with excellent catalytic activity for methylene blue. *Polyhedron*, **160**, 229–237.
- Huang, L., Wang, S.S., Zhao, J.W., Cheng, L., Yang, G.Y., 2014. Synergistic combination of multi-ZrIV cations and lacunary keggin germanotungstates leading to a gigantic Zr₂₄-cluster-substituted polyoxometalate. *J. Am. Chem. Soc.*, **136**, 7637–7642.
- Kastner, K., Kibler, A.J., Karjalainen, E., Fernandes, J.A., Sans, V. and Newton, G.N., 2017. Redox-active organic–inorganic hybrid polyoxometalate micelles. *Journal of Materials Chemistry A*, **5**, 11577–11581.
- Lan, Q., Zhang, J., Zhang, Z.M., Lu, Y., Wang, E.B., 2013. Two three-dimensional porous frameworks built from metal–organic coordination polymer sheets pillared by polyoxometalate clusters. *Dalton Transactions*, **42**, 16602–16607.
- Liu, J., Zhang, Y., Shang, S., Li, Y., Chen, L. and Zhao, J., 2015. Syntheses, structures and properties of three metal–organic complexes containing 2,2'-dipyridyl-5,5'-dicarboxylate ligands. *Journal of Solid State Chemistry*, **221**, 5–13.
- Lu, X.X., Luo, Y.H., Xu, Y., Zhang, H., 2015. Temperature-dependent assembly of two 3D $[BW_{12}O_{40}]^{5-}$ -based coordination polymers with visible light driven photocatalytic properties. *CrystEngComm*, **17**, 1631–1636.
- Lu, Y.K., Li, Y.P., Yang, Y.L., Wang, W.H., Pan, Y., Yan, W.F., Liu, Y.Q., 2019. Modified polyoxometalate: a novel monocapped bi-supporting and reduced α -Keggin structure $\{PMo_{12}O_{40}[Cu(2,2'-bpy)]\}[Cu(2,2'-bpy)(en)(H_2O)]_2$. *Acta Crystallographica Section C*, **C75**, 1344–1352.
- Shakeri, A., Mighani, H., Salari, N. and Salehi, H., 2019. Surface modification of forward osmosis membrane using polyoxometalate based open frameworks for hydrophilicity and water flux improvement. *Journal of Water Process Engineering*, **29**, 100762.
- Sheldrick, G.M., 2008. A short history of SHELX. *Acta Crystallographica Section A*, **A64**, 112–122.
- Sheldrick, G.M., 2015. Crystal structure refinement with SHELXL. *Acta Crystallographica Section C*, **C71**, 3–8.
- Xiao, L.N., Yang, L.X., Du, X.D., Lan, Q., Zhang, H. and Cui, X.B., 2018. Four new compounds based on Keggin polyoxotungstates and transition metal complexes. *Polyhedron*, **147**, 42–48.
- Zhang, J., Song, Y.F., Cronin, L. and Liu, T., 2008. Self-Assembly of Organic–Inorganic Hybrid Amphiphilic Surfactants with Large Polyoxometalates as Polar Head Groups. *Journal of the American Chemical Society*, **130(44)**, 14408–14409.
- Zhao, W., Cui, J., Hao, J. and Horn, J.D.V., 2019. Co-assemblies of polyoxometalate $\{Mo_{72}Fe_{30}\}$ /double-tailed magnetic-surfactant for magnetic-driven anchorage and enrichment of protein. *Journal of Colloid and Interface Science*, **536**, 88–97.
- Zheng, S.T., Yuan, D.Q., Jia, H.P., Zhang, J., Yang, G.Y., 2007. Combination between lacunary polyoxometalates and high-nuclear transition metal clusters under hydrothermal conditions: I. From isolated cluster to 1-D chain. *Chem. Commun.*, **18**, 1858–1860.
- Zheng, S.T., Yang, G.Y. 2012. Recent advances in paramagnetic-TM-substituted polyoxometalates (TM = Mn, Fe, Co, Ni, Cu). *Chem. Soc. Rev.*, **41**, 7623–7646.
- Zong, L., Wu, H., Lin, H. and Chen, Y., 2018. A polyoxometalate-functionalized two-dimensional titanium carbide composite MXene for effective cancer theranostics. *Nano Research*, **11**, 4149–4168.

İnternet kaynakları

1-Mercury, version 3.3; CCDC, available online via ccdc.cam.ac.uk/products/mercury.